



Original Article

SPECT imaging evaluation of ^{111}In -chelated cetuximab for diagnosing EGFR-positive tumor in an HCT-15-induced colorectal xenograft

Bin-Bin Shih^a, Yi-Fang Chang^b, Chun-Chia Cheng^b, Hao-Jhih Yang^c, Kang-Wei Chang^c,
Ai-Sheng Ho^a, Hua-Ching Lin^d, Chun Yeh^a, Chun-Chao Chang^{e,f,*}

^a Division of Gastroenterology, Cheng Hsin General Hospital, Taipei, Taiwan, ROC

^b Hematology and Oncology, Mackay Memorial Hospital, Taipei, Taiwan, ROC

^c Institute of Nuclear Energy Research, Atomic Energy Council, Taoyuan, Taiwan, ROC

^d Division of Proctology, Cheng Hsin General Hospital, Taipei, Taiwan, ROC

^e Division of Gastroenterology and Hepatology, Department of Internal Medicine, Taipei Medical University Hospital, Taipei, Taiwan, ROC

^f Division of Gastroenterology and Hepatology, Department of Internal Medicine, School of Medicine, College of Medicine, Taipei Medical University, Taipei, Taiwan, ROC

Received September 9, 2016; accepted February 8, 2017

Abstract

Background: Epidermal growth factor receptor (EGFR) overexpressed in colorectal cancer (CRC) is a tumor target for developing the anti-tumor theranostic agents. Cetuximab, an anti-EGFR monoclonal antibody against EGFR-positive tumors, inhibits cell proliferation and growth was labeled with radioactive ^{111}In (^{111}In) in this study for diagnosing EGFR-positive CRC. The aim of this study was to evaluate the efficacy of noninvasive nuclear imaging agent ^{111}In -cetuximab and investigate the biological distribution of ^{111}In -cetuximab in the HCT-15-induced EGFR-positive CRC tumor xenografts.

Methods: We conjugated cetuximab with an isotope chelator, diethylene triamine penta acetic acid (DTPA), and consequently labeled cetuximab-DTPA with ^{111}In and measured the labeling efficacy by an instant thin layer chromatography (iTLC). Furthermore, the ^{111}In -cetuximab was investigated and compared for imaging small (50 mm^3) and large (250 mm^3) tumor of CRC xenografts, respectively.

Results: The conjugated ratio between cetuximab and DTPA was 1:6 measured by MALDI-TOF-MS. The better labeling concentration of cetuximab with 10 mCi of ^{111}In was calculated and experimented as 48 μg , resulting in labeling efficacy >80% detected by iTLC. The results revealed that the ^{111}In -cetuximab accumulated in the both sizes of tumors as a reliable noninvasive diagnostic agent, whereas the ratio of tumor to muscle in the large tumor was 7.5-fold. The biodistribution data indicated that the ^{111}In -cetuximab bound to tumor specifically that was higher than that in other organs.

Conclusion: We suggested that the ^{111}In -cetuximab was potential for early diagnosis and prognostic monitor of EGFR-positive CRC in further clinical practice.

Copyright © 2017, the Chinese Medical Association. Published by Elsevier Taiwan LLC. This is an open access article under the CC BY-NC-ND license (<http://creativecommons.org/licenses/by-nc-nd/4.0/>).

Keywords: Cetuximab; Colorectal adenocarcinoma; Epidermal growth factor receptor; ^{111}In

1. Introduction

Colorectal cancer (CRC) such as adenocarcinoma occurred with high incidence worldwide belonging to a malignant tumor, which is diagnosed without major symptom at an early stage. Almost 60% of CRC occurs in the developed countries.¹ Since early diagnosis of CRC improves the outcome of

Conflicts of interest: The authors declare that they have no conflicts of interest related to the subject matter or materials discussed in this article.

* Corresponding author. Dr. Chun-Chao Chang, Division of Gastroenterology, Taipei Medical University Hospital, 250, Wu-Hsing Street, Taipei 110, Taiwan, ROC.

E-mail address: chunchao@tmu.edu.tw (C.-C. Chang).

<http://dx.doi.org/10.1016/j.jcma.2017.02.010>

1726-4901/Copyright © 2017, the Chinese Medical Association. Published by Elsevier Taiwan LLC. This is an open access article under the CC BY-NC-ND license (<http://creativecommons.org/licenses/by-nc-nd/4.0/>).

therapeutic treatment for CRC,² it is urgent to develop a reliable and early CRC diagnostic agent. Moreover, CRC is always diagnosed occurring in late stage with metastasis, but the current diagnosing standard, colonoscopy with the histopathologic examination, is insufficient to detect the early tumor and metastasis.

Epidermal growth factor receptor (EGFR) overexpresses in the tissues of CRC by 97% as a cell membrane protein participating in cell proliferation.^{3,4} Literature has indicated that EGFR is a tumor target of CRC.^{5–7} A previous study has developed EGFR-targeted therapeutic antibodies against CRC such as cetuximab⁸ which is a chimeric monoclonal antibody. Besides, cetuximab is also utilized as a targeting probe carrying various diagnostic and therapeutic agents.^{9–11} The CRC diagnosis based on the use of cetuximab is proven a promising strategy for noninvasively tracking tumor locations and monitoring the therapeutic effects.

Compared to the gold standard, colonoscopy with histopathologic examination, in diagnosing CRC, the noninvasive nuclear imaging techniques such as single-photon emission computerized tomography/computer tomography (SPECT/CT) or positron emission tomography/computer tomography (PET/CT) provide higher sensitive diagnostic resolution and wide-screen for whole tissues in body specimen,^{12–14} suggesting that early tumor diagnosis and metastasis diagnosis by nuclear imaging techniques are feasible. Based on the concept of nuclear imaging methodology, this study aimed to evaluate the noninvasive nuclear imaging technique for diagnosing EGFR-positive CRC using a radioactive isotope-chelated-cetuximab, which may provide an evidence for the consequent utilization of EGFR-specific anti-tumor therapy.

In this study, we intended to label cetuximab with ¹¹¹In-dium (¹¹¹In) (half-life = 2.83 days, r -ray = 0.2454 MeV) through diethylene triamine penta acetic acid (DTPA) chelator. The optimal labeling ratio was calculated and experimentally investigated. The cell binding of cetuximab-DTPA to EGFR-positive HCT-15 cells was investigated. The reliability of nuclear imaging diagnosis using ¹¹¹In-cetuximab was demonstrated in the HCT-15-induced tumor xenografts which carrying small (50 mm³) and large (250 mm³) tumors individually. Furthermore, the biodistribution of ¹¹¹In-Cetuximab in tumor xenografts was also investigated.

2. Methods

2.1. HCT-15 culture and tumor xenograft model

Human colorectal carcinoma cells (HCT-15) were purchased from the American Type Culture Collection (ATCC) and cultured in F12K medium with 10% of fetal bovine serum. HCT15 is an EGFR-positive colorectal cancer cell line with KRAS mutation¹⁵ which model is similar to a previous study utilizing HCT116 for EGFR-nuclear imaging.¹⁰ All cells were incubated at 37 °C and 5% CO₂. Male nude mice were purchased from BioLASCO Taiwan Co., Ltd, Taiwan. The 5-week-old mice were housed in a 12 h-light cycle at 22 °C. The animal studies were approved by the institutive ethical

review committee in Institute of Nuclear Energy Research, Taiwan, which followed the NIH guidelines on the care and welfare of laboratory animals. HCT-15 cells (2×10^6) were subcutaneously (s.c.) inoculated into the right leg of nude mice. Tumors were established for 7 days as the small tumor model (50 mm³), and 30 days as the large tumor model (250 mm³) before the tumor imaging.

2.2. Conjugation and measurement of cetuximab-DTPA

To create cetuximab-DTPA, cetuximab was incubated with P-SCN-Bn-DTPA (w/w 1:10, Macrocylics, Dallas, TX, USA) in carbonate-bicarbonate buffer (pH 9.0) at room temperature for 2 h. The cetuximab-conjugated DTPA was purified using G-25 column, whereas the second ml was collected. The cetuximab and cetuximab-DTPA were added with an equal volume of sinapinic acid (20 mg/ml in 50% acetonitrile/0.5% TFA) and dried on a steel plate. The molecular weights of antibodies were analyzed using matrix-assisted laser desorption/ionization time-of-flight mass spectrometry (MALDI-TOF-MS, UltraflexIII, Bruker Daltonics GmbH, Germany).

2.3. Cetuximab-DTPA binding assay

Each HCT-15 cells (2×10^6 cells) were treated with 1 µg/ml of cetuximab-FITC for 30 min at room temperature. The 20-fold of cetuximab or cetuximab-DTPA higher than cetuximab-FITC was added simultaneously for investigating the competing capacity. After the reaction, the medium was removed and washed using phosphate-buffered saline (PBS) for three times. The cells in PBS buffer were analyzed using FACSCalibur Flow Cytometer (BD Bioscience, USA).

2.4. The labeling of ¹¹¹In-cetuximab in vitro

First, the cetuximab-DTPA was mixed and incubated with ¹¹¹In by 1:1 molar ratio. The specific radioactivity (SRA) of ¹¹¹In was calculated as following formula: SRA (Bq/g) = $\lambda N = 0.693/\text{half-life of } ^{111}\text{In (seconds)} \times 6.03 \times 10^{23}/\text{MW} = 1.51351 \times 10^{16}$. Therefore, 10 mCi of ¹¹¹In = $3.7 \times 10^8 \text{ Bq}/1.51351 \times 10^{16} = 2.445 \times 10^{-2} \mu\text{g}$. According to the calculated results, the cetuximab-DTPA incubated with 10 mCi of ¹¹¹In was $2.445 \times 10^{-2} \mu\text{g}/111 \times 156176 = 34.4 \mu\text{g}$ by 1:1 molar ratio. Since the conjugated ratio between cetuximab and DTPA was measured 1:6, we expected that 5.73 µg of cetuximab could be labeled with 10 mCi of ¹¹¹In molecules. In experiments, we incubated 3, 6, 12, 24, 48, 96, 192, 384, and 768 µg of cetuximab-DTPA with 10 mCi of ¹¹¹In, respectively, for 30 min and 24 h in PBS buffer, pH7.4. This experiment was performed just once for reason of as low as reasonably achievable (ALARA), however, the labeling rate was measured every time when applying in animal nuclear imaging. The labeling rate >80% was acceptable as performed in the tumor xenografts. The labeling efficiency was measured using instant thin layer chromatography (iTLC) on the silica gel impregnated glass fiber sheets (PALL corporation, USA), whereas PBS was used as the

mobile phase. Then, the sheets were measured using a radioactive scanner (AR-2000radio-TLC Imaging Scanner, Bioscan, France).

2.5. Nuclear imaging and biodistribution in HCT-15-induced tumor xenografts

The HCT-15-induced tumor xenografts were intravenously injected with ^{111}In -cetuximab ($n = 3$) or ^{111}In alone ($n = 3$) by 1 mCi of radioactivity for each mouse. A Nano-SPECT/CT (Mediso Medical Imaging Systems, USA) was utilized to detect and image the tumors in the tumor model *in vivo*. For investigating the biodistribution of ^{111}In -cetuximab in EGFR-positive HCT-15-induced xenografts, the organs were harvested and measured the radioactivity using a gamma counter (1470 WIZARD, PerkinElmer, USA) after the agents and ^{111}In injection for 48 h. The percent injected dose per gram of tissue (%ID/g) was utilized to represent the radioactive intensity in each collected organ.

2.6. Statistical analysis

Statistical analysis was performed using GraphPad Prism V5.01 software (GraphPad Software, Inc., California, USA). All analysis data with more than two groups were performed by ANOVA followed by posthoc analysis with Bonferroni's test. Student's *t*-test was used to compare two groups. The significance difference was acceptable as $p < 0.05$.

3. Results

3.1. Cetuximab specifically bound to EGFR-overexpressed HCT-15 cells

To investigate EGFR expression in colorectal HCT-15 cancer cells, cetuximab was labeled with fluorescent FITC, and then the agent was purified using a G-25 column. HCT-15 cells were treated and incubated with none, 1 $\mu\text{g}/\text{ml}$ of cetuximab-FITC, or 1 $\mu\text{g}/\text{ml}$ of cetuximab-FITC plus 10 $\mu\text{g}/\text{ml}$ of cetuximab, respectively, for 30 min at room temperature. We figured out that the fluorescent intensity in the cetuximab-FITC group was higher than that in other groups (Fig. 1A and B), revealing that cetuximab specifically bound to HCT-15 cells which overexpressed EGFR.¹⁵

3.2. Cetuximab-DTPA bound to HCT-15 cells

Cetuximab was labeled with ^{111}In through DTPA chelator, therefore, we first conjugated cetuximab with DTPA. We added excess DTPA to cetuximab by 10-fold for maximally conjugating DTPA to available amide groups of cetuximab. MALDI-TOF MS results showed that the molecular weight 152,153Da of cetuximab shifted as 156,176Da (Fig. 2A), indicating that the conjugated ratio was approximately 1:6 between cetuximab and DTPA. In order to investigate the binding capacity of cetuximab-DTPA to HCT-15 cells, 10 $\mu\text{g}/\text{ml}$ of cetuximab-DTPA was added with 1 $\mu\text{g}/\text{ml}$ of

cetuximab-FITC as a competitor. We found that cetuximab-DTPA reduced the binding capacity of cetuximab-FITC to HCT-15 cells (Fig. 2B and C), revealing that cetuximab-DTPA still had the binding capacity to EGFR on HCT-15 cells.

3.3. The optimal labeling ratio of cetuximab-DTPA with ^{111}In

The theoretical labeling concentration of cetuximab-DTPA with ^{111}In is 5.73 μg of cetuximab-DTPA to 10 mCi of ^{111}In described in Methods and Materials. We intended to evaluate the accurate labeling ratio experimentally, 3, 6, 12, 24, 48, 96, 192, 384, 768 μg of cetuximab-DTPA were incubated with 10 mCi of ^{111}In , respectively. We found that the amount of cetuximab-DTPA over 48 μg resulted in >80% labeling efficiency (Fig. 3A and B), indicating that the optimal labeling concentration was 48 μg of cetuximab-DTPA to 10 mCi of ^{111}In corresponding to the theoretical calculation. The labeling efficiency of ^{111}In -cetuximab was measured >80% in 24 h (Fig. 3A), revealing that ^{111}In -cetuximab was stable.

3.4. ^{111}In -cetuximab nuclear imaging and biodistribution

Since ^{111}In -cetuximab was created, we applied ^{111}In -cetuximab to detect the EGFR-positive tumors in the HCT-15-induced xenografts. The ^{111}In -cetuximab was injected in the tumor models implanted with a small tumor (50 mm^3) and large tumor (250 mm^3) and consequently imaged using a Nano-SPECT/CT device. We found that ^{111}In -cetuximab accumulated in the mouse liver and tumor in 24 h post injection, including small and large tumors (Fig. 4A and B). Otherwise, ^{111}In accumulated in kidney majorly. The radioactivity of ^{111}In -cetuximab in the tumor was higher in small or large tumor model compared to control group. Next, the biodistribution of ^{111}In -cetuximab was investigated compared to that of ^{111}In . The results were consistent with the SPECT/CT images showing the higher radioactivity in tumors compared to other organs in the ^{111}In -cetuximab-injected large tumor xenografts (Fig. 5B). Otherwise, ^{111}In majorly distributed in the kidney (Fig. 5A). The tumor to muscle ratio of ^{111}In -cetuximab was measured 7.5-fold which was higher than that of ^{111}In group measured as 3.1-fold (Fig. 5C), indicating that ^{111}In -cetuximab specifically bound to EGFR-positive tumors as a reliable diagnosing agent. Meanwhile, the sum of radioactivity in ^{111}In group was higher than that in the ^{111}In -cetuximab group (Fig. 5D). The result indicated that ^{111}In labeled with cetuximab through chelator DTPA was easily excreted out the mice better than free ^{111}In , suggesting that this labeling method may not lead to accumulation of ^{111}In metal in mice.

4. Discussion

EGFR overexpresses in a variety of cancers, including CRC,^{3,16} head and neck cancer,¹⁷ lung cancer.^{18,19} Therefore, diagnosing the EGFR-positive tumor is an important issue for

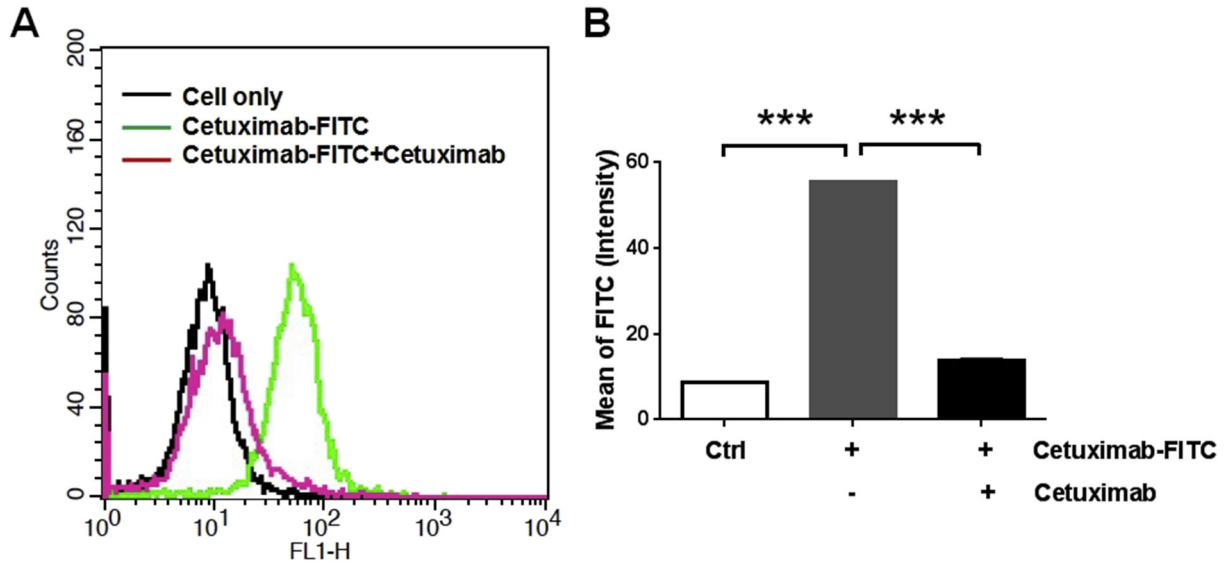


Fig. 1. Overexpression of EGFR was recognized by cetuximab in colorectal HCT-15 cells. To make sure the overexpression of EGFR in HCT-15 cells, and the binding capacity of cetuximab to HCT-15 cells, cetuximab-FITC was utilized and incubated with HCT-15 cells. (A & B) The higher binding capacity was found in cetuximab-FITC (1 μ g/ml) group measured using a flow cytometry technique, which was blocked when the 10-fold of cetuximab was added. *** $p < 0.001$.

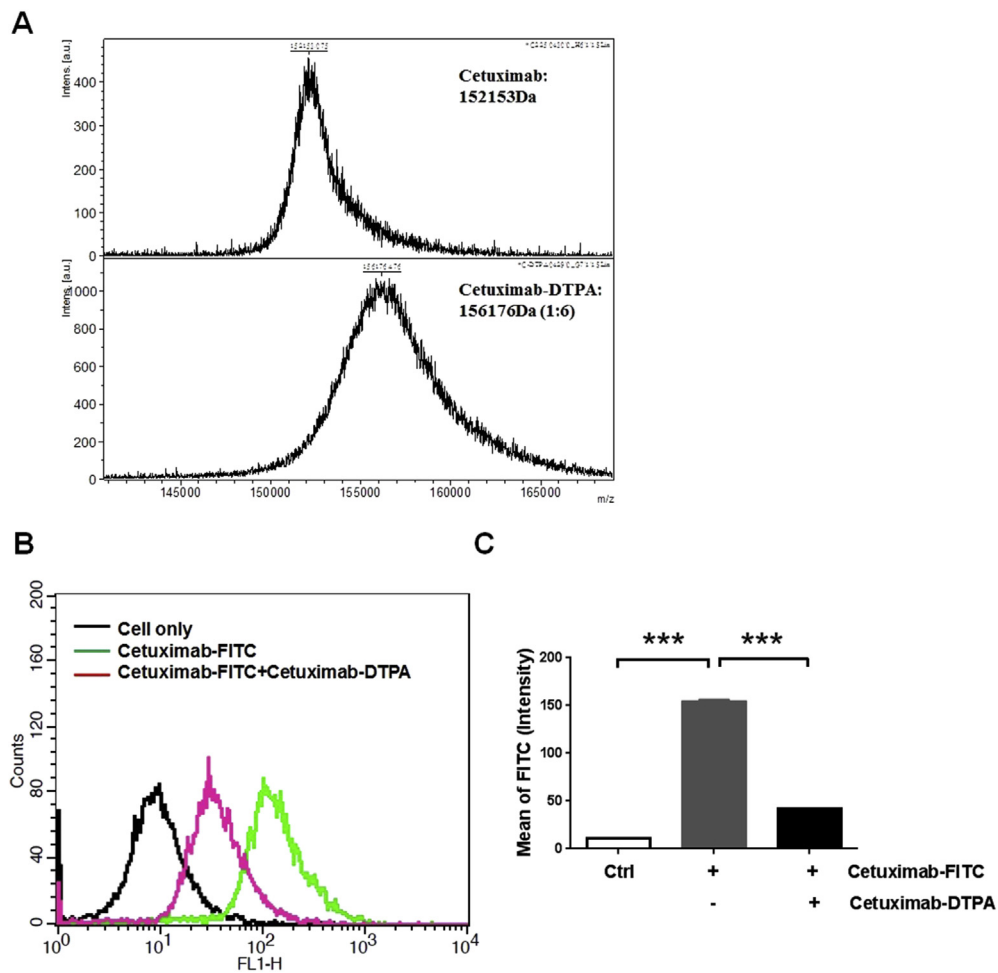


Fig. 2. The ratio of cetuximab to DTPA was 1:6. (A) Cetuximab was conjugated with *p*-SCN-Bn-DTPA for exact 2 h, which was measured using MALDI-TOF MS. The molecular weight of cetuximab was measured 152,153Da and shifted as 156,176Da after DTPA (649.9Da) conjugation. The ratio was estimated 1:6 between cetuximab and DTPA. (B&C) The cetuximab-DTPA was used as a competitor against cetuximab-FITC for determining the binding capacity of cetuximab-DTPA. The 10-fold of cetuximab-DTPA significantly blocked the binding capacity of cetuximab-FITC to HCT-15 cells detected using a flow cytometry technique. *** $p < 0.001$.

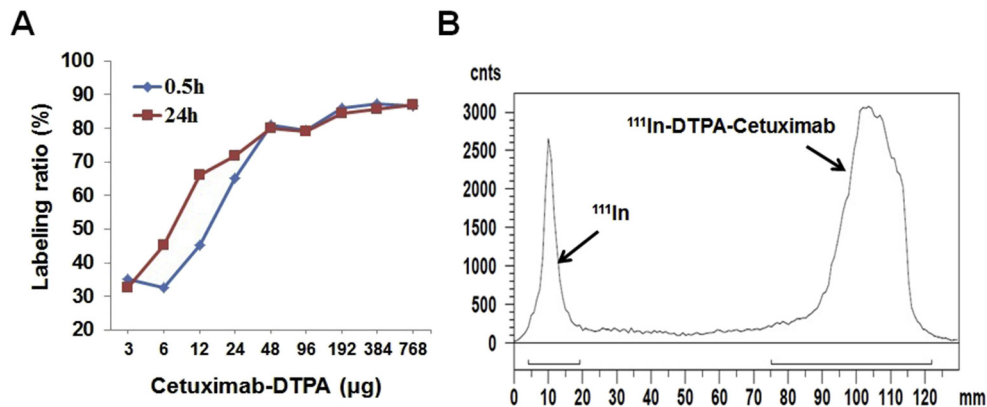


Fig. 3. Labeling of cetuximab-DTPA with radioactive ^{111}In . Theoretically, 10 mCi of ^{111}In was labeled with 34.4 μg of cetuximab by 1:1 molar ratio described in Methods and Materials. (A) In the experiment, a wide range of cetuximab-DTPA (3–768 μg) was incubated with 10 mCi of ^{111}In , respectively. The labeling efficiency was determined using iTLC. The higher amount of cetuximab-DTPA increased the labeling efficiency, but the limit was around 80% shown by the arrow whereas 48 μg of cetuximab-DTPA was incubated with 10 mCi of ^{111}In both for 0.5 h or 24 h. (B) The iTLC result indicated that 48 μg of cetuximab-DTPA were incubated with 10 mCi of ^{111}In for 0.5 h demonstrated the successful labeling.

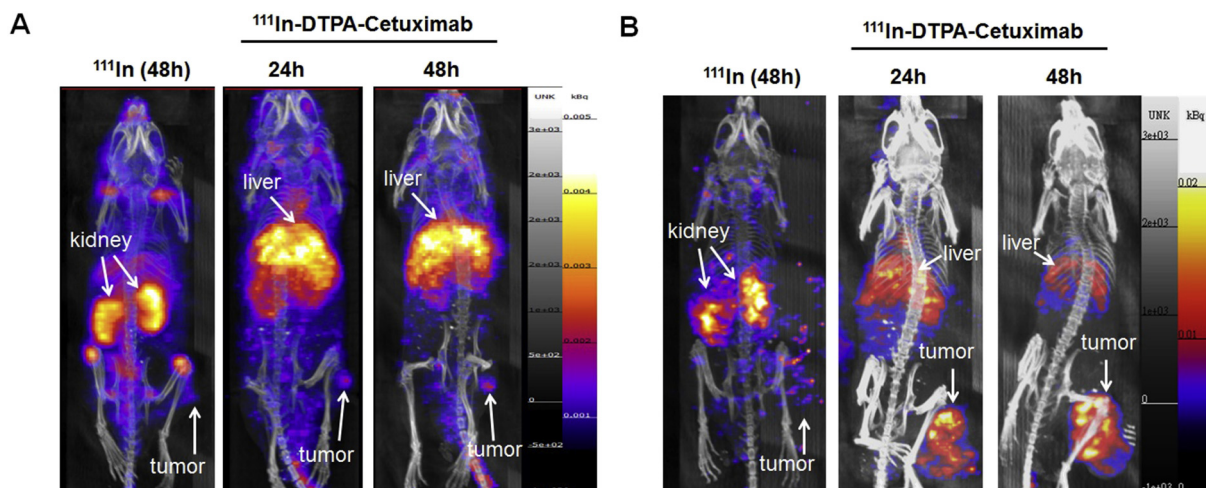


Fig. 4. ^{111}In -cetuximab was utilized to diagnose early and advanced colorectal cancer in HCT-15-induced xenografts. (A) The early tumors ($n = 3$) implanted in nude mice for 1 week (50 mm^3) were detected using ^{111}In -cetuximab cooperated with SPECT/CT. The radioactive image in the tumor of the ^{111}In -cetuximab group was apparently observed both in 24 h and 48 h and higher than that in the ^{111}In group. ^{111}In -cetuximab majorly accumulated in liver and tumor, otherwise, ^{111}In accumulated only in the kidney. (B) The advanced tumor (250 mm^3 , $n = 3$) was established and imaged. The tumors in the ^{111}In -cetuximab group were apparently detected and imaged, and radioactive signals were higher than that in the ^{111}In group.

selecting the adequate therapy. In this study, we intended to label cetuximab with radioactive ^{111}In and to optimize the labeling condition for creating ^{111}In -cetuximab serving as a diagnostic imaging tool for CRC. Our results demonstrated that ^{111}In -cetuximab specifically targeted to EGFR-positive HCT-15-induced tumors, and the optimal labeling concentration was 48 μg of cetuximab with 10 mCi of ^{111}In . This research provided the manufactured condition for EGFR nuclear imaging agent, ^{111}In -cetuximab.

Targeting to EGFR based on its specific antibody is useful and potential for developing the diagnostic methodology for EGFR-positive tumors. Since utilization of radiolabeled cetuximab has been applied for diagnosing tumors such as CRC²⁰ or head and neck tumor,²¹ to investigate and optimize the labeling ratio between cetuximab and isotope was needed. Although the labeling efficiency was limited around 80%

when using 48 μg of cetuximab incubated with 10 mCi of ^{111}In , the EGFR-positive tumor was clearly imaged and diagnosed. The higher amount of cetuximab with 10 mCi of ^{111}In led to increased labeling efficiency, however, the unlabeled cetuximab played as a competitor blocking the binding of ^{111}In -cetuximab similar to a study published by Nayak et al. using co-injection of cetuximab with ^{86}Y -labeled cetuximab.²² Therefore, finding the optimal radio-labeled rate is necessary for improving the radio-imaging signals. Previously, Shih et al. have utilized 100 μg of cetuximab to label with 10 mCi of ^{111}In , resulting in similar radio-labeled rate (~80%).¹⁰ Although the radio-labeled rate >80% is acceptable for a nuclear imaging application, the extra unlabeled cetuximab may reduce the radioactive signals in real practice, leading to lower resolution of nuclear imaging. According to their data, they have declared that ^{111}In -cetuximab leads to highest

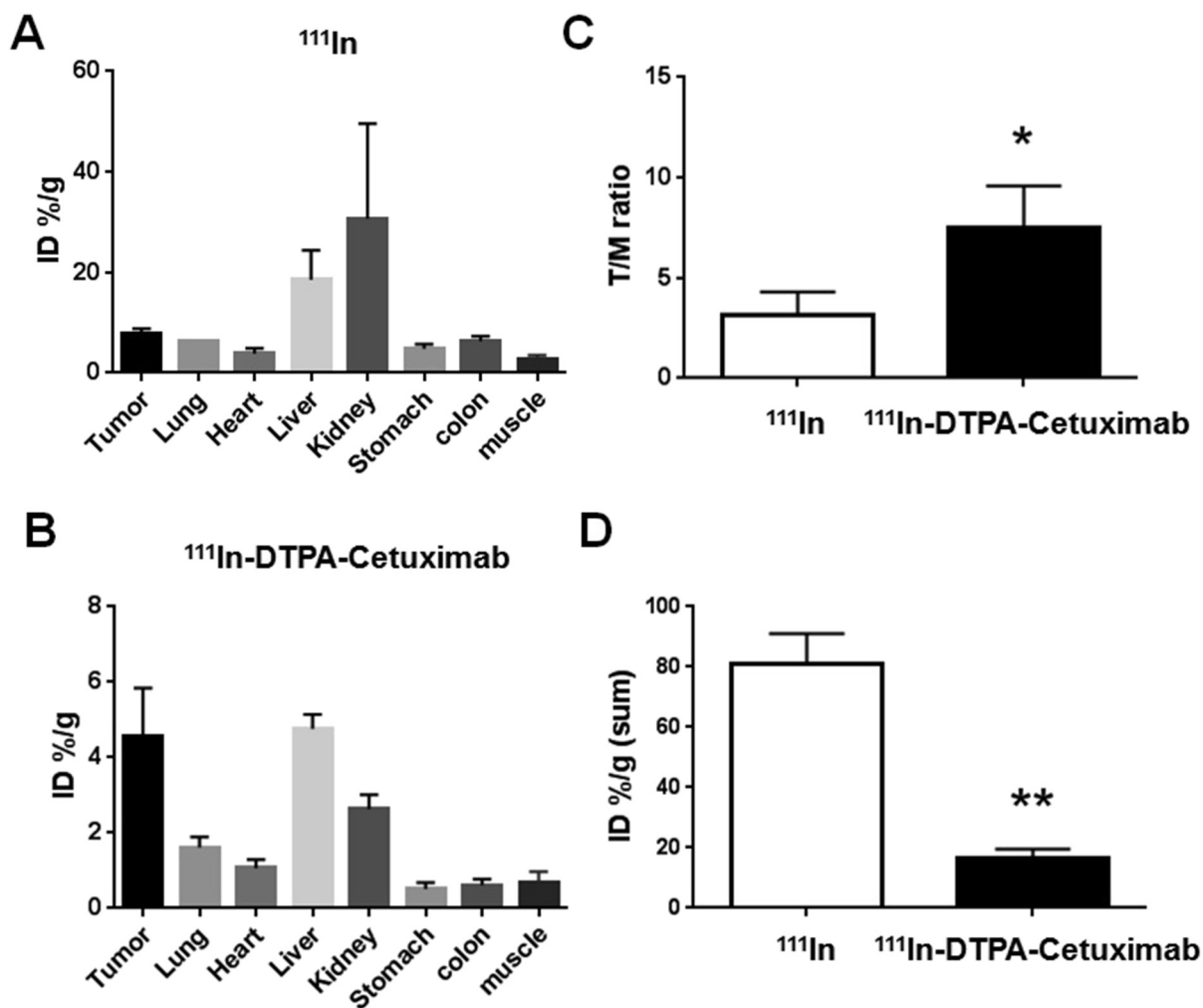


Fig. 5. Biodistribution of ^{111}In -cetuximab in the HCT-15-induced xenografts. (A) Biodistribution of ^{111}In in tumor xenografts was investigated. The results indicated ^{111}In accumulated highest in kidney and liver rather than that in the tumor. (B) The result revealed that ^{111}In -cetuximab apparently targeted and accumulated in tumor higher than that in other organs except for liver. (C) The tumor to muscle (T/M) ratio was compared and investigated. The T/M ratio of ^{111}In -cetuximab was higher than that of ^{111}In . (D) The sum of radioactivity in the collected organs was significantly reduced in the ^{111}In -cetuximab group compared to ^{111}In group, indicating that ^{111}In -cetuximab rapidly excreted from the tumor xenograft mice. * $p < 0.05$. ** $p < 0.01$.

radioactive signals in 72 h after injection by tail vein. However, we not only detected the HCT-15-derived large tumors in 24 h but also detected the small tumors, implying the optimal labeling ratio was significant for nuclear imaging. Therefore, in order to obtain a better and higher radioactive imaging, we suggested that the labeling ratio: 48 μg of cetuximab with 10 mCi of ^{111}In was adequate.

Currently, cetuximab has been labeled with ^{111}In ,^{10, 23} ^{89}Zr ,^{24, 25} ^{64}Cu ,^{26,27} and $^{99\text{m}}\text{Tc}$.²⁸ The half-life of $^{99\text{m}}\text{Tc}$ is 6 h, which is not enough applied in antibody-based nuclear imaging such as cetuximab with the apparent imaging signals after 24 h injection. ^{89}Zr and ^{64}Cu are PET isotopes having higher resolution than SPECT imaging such as images derived from ^{111}In .²⁹ ^{64}Cu (half-life: 12.7 h) is potential for applying not only in diagnostic imaging but also for targeted radiotherapy due to the additional β^- particles emitting. Because the half-life of circulation of antibody in the biologic body was over 63 h, and the highest imaging intensity of antibody appears after 48 h injection, ^{89}Zr (half-life: 3.3day) and ^{111}In

(half-life: 2.8day) are more suitable to label with cetuximab. No matter what radioactive isotopes are selected to label with cetuximab, the optimal labeling ratio is equivalent to the result demonstrated in this study.

^{111}In -cetuximab was demonstrated to diagnose an early small tumor and advanced large tumor in this study. Due to the labeling of isotope was through DTPA chelator, further radiotherapy using β^- -emitted yttrium-90 (^{90}Y through DTPA) chelating is feasible.^{30–32} ^{90}Y -cetuximab combined with external irradiations had been demonstrated to reduce tumor size in a 3D cell assay.³³ Moreover, ^{111}In -cetuximab may be used to diagnose the prognosis of chemotherapy, tumor metastasis, and the cetuximab-derived resistance. This study addressed and evaluated the correct labeling ratio, nuclear imaging, and biodistribution of ^{111}In -cetuximab.

Beside tumors, ^{111}In -cetuximab was also highly accumulated in the liver which also overexpresses EGFR.³⁴ The biodistribution results indicated the equal radioactive intensity between tumor and liver in a large tumor model in 48 h. Since

existed location of the colon is distinguished from the liver, the nuclear imaging of CRC using ^{111}In -cetuximab may be not interfered by that from the liver. However, the acute toxicity in the liver is needed to be monitored in the performance of ^{111}In -cetuximab, particularly in the patients with liver diseases. Moreover, for detecting the tumor metastasis in the liver, this nuclear imaging technique based on ^{111}In -cetuximab is inadequate. Other techniques are needed for assisting the diagnosis of tumor metastasis in liver.

In conclusion, we evaluated that ^{111}In -cetuximab was useful for detecting an EGFR-positive tumor, and optimized the labeling ratio between cetuximab and radioactive ^{111}In . The theoretically labeling ratio was equivalent to the experimental result, which may be applied in another labeling pair of antibody and isotope. We suggest that optimal labeling of ^{111}In -cetuximab can be used to diagnose EGFR-positive CRC.

Acknowledgments

This study was supported by the grant ARA010201 from Atomic Energy Council of Republic of China, and the grant 104-03 from Cheng Hsin General Hospital.

References

1. Ferlay J, Shin HR, Bray F, Forman D, Mathers C, Parkin DM. Estimates of worldwide burden of cancer in 2008: GLOBOCAN 2008. *Int J Cancer* 2010;**127**:2893–917.
2. Benson 3rd AB. Epidemiology, disease progression, and economic burden of colorectal cancer. *J Manag Care Pharm* 2007;**13**:S5–18.
3. Spano JP, Lagorce C, Atlan D, Milano G, Domont J, Benamouzig R, et al. Impact of EGFR expression on colorectal cancer patient prognosis and survival. *Ann Oncol* 2005;**16**:102–8.
4. Penault-Llorca F, Bibeau F, Arnould L, Bralet MP, Rochaix P, Sabourin JC. [EGFR expression in colorectal cancer and role in tumorigenesis]. *Bull Cancer* 2005;**92**:S5–11.
5. Markman B, Javier Ramos F, Capdevila J, Tabernero J. EGFR and KRAS in colorectal cancer. *Adv Clin Chem* 2010;**51**:71–119.
6. Overman MJ, Hoff PM. EGFR-targeted therapies in colorectal cancer. *Dis Colon Rectum* 2007;**50**:1259–70.
7. Messersmith WA, Ahnen DJ. Targeting EGFR in colorectal cancer. *N Engl J Med* 2008;**359**:1834–6.
8. Wong SF. Cetuximab: an epidermal growth factor receptor monoclonal antibody for the treatment of colorectal cancer. *Clin Ther* 2005;**27**:684–94.
9. Zalba S, Contreras AM, Haeri A, Ten Hagen TL, Navarro I, Koning G, et al. Cetuximab-oxaliplatin-liposomes for epidermal growth factor receptor targeted chemotherapy of colorectal cancer. *J Control Release* 2015;**210**:26–38.
10. Shih YH, Peng CL, Lee SY, Chiang PF, Yao CJ, Lin WJ, et al. ^{111}In -cetuximab as a diagnostic agent by accessible epidermal growth factor (EGF) receptor targeting in human metastatic colorectal carcinoma. *Oncotarget* 2015;**6**:16601–10.
11. Sihver W, Pietzsch J, Krause M, Baumann M, Steinbach J, Pietzsch HJ. Radiolabeled cetuximab conjugates for EGFR targeted cancer diagnostics and therapy. *Pharm (Basel)* 2014;**7**:311–38.
12. Sumi Y, Ozaki Y, Shindoh N, Kyogoku S, Katayama H. Usefulness of thallium-201 SPECT imaging for the evaluation of local recurrence of colorectal cancer. *Ann Nucl Med* 1998;**12**:191–5.
13. Meinel FG, Schramm N, Haug AR, Graser A, Reiser MF, Rist C. [Importance of PET/CT for imaging of colorectal cancer]. *Radiologe* 2012;**52**:529–36.
14. Bamba Y, Itabashi M, Kameoka S. Value of PET/CT imaging for diagnosing pulmonary metastasis of colorectal cancer. *Hepatogastroenterology* 2011;**58**:1972–4.
15. Troiani T, Napolitano S, Vitagliano D, Morgillo F, Capasso A, Sforza V, et al. Primary and acquired resistance of colorectal cancer cells to anti-EGFR antibodies converge on MEK/ERK pathway activation and can be overcome by combined MEK/EGFR inhibition. *Clin Cancer Res* 2014;**20**:3775–86.
16. Saif MW. Colorectal cancer in review: the role of the EGFR pathway. *Expert Opin Investig Drugs* 2010;**19**:357–69.
17. Keren S, Shoude Z, Lu Z, Beibei Y. Role of EGFR as a prognostic factor for survival in head and neck cancer: a meta-analysis. *Tumour Biol* 2014;**35**:2285–95.
18. Hirsch FR, Varella-Garcia M, Cappuzzo F. Predictive value of EGFR and HER2 overexpression in advanced non-small-cell lung cancer. *Oncogene* 2009;**1**(Suppl. 28):S32–7.
19. Mukohara T, Kudoh S, Yamauchi S, Kimura T, Yoshimura N, Kanazawa H, et al. Expression of epidermal growth factor receptor (EGFR) and downstream-activated peptides in surgically excised non-small-cell lung cancer (NSCLC). *Lung Cancer* 2003;**41**:123–30.
20. Goetz M, Hoetker MS, Diken M, Galle PR, Kiesslich R. In vivo molecular imaging with cetuximab, an anti-EGFR antibody, for prediction of response in xenograft models of human colorectal cancer. *Endoscopy* 2013;**45**:469–77.
21. van Dijk LK, Hoeben BA, Kaanders JH, Franssen GM, Boerman OC, Bussink J. Imaging of epidermal growth factor receptor expression in head and neck cancer with SPECT/CT and ^{111}In -labeled cetuximab-F(ab')₂. *J Nucl Med* 2013;**54**:2118–24.
22. Nayak TK, Regino CA, Wong KJ, Milenic DE, Garmestani K, Baidoo KE, et al. PET imaging of HER1-expressing xenografts in mice with ^{86}Y -CHX-A'-DTPA-cetuximab. *Eur J Nucl Med Mol Imaging* 2010;**37**:1368–76.
23. Hoeben BA, Molkenboer-Kuonen JD, Oyen WJ, Peeters WJ, Kaanders JH, Bussink J, et al. Radiolabeled cetuximab: dose optimization for epidermal growth factor receptor imaging in a head-and-neck squamous cell carcinoma model. *Int J Cancer* 2011;**129**:870–8.
24. Makris NE, Boellaard R, van Lingen A, Lammertsma AA, van Dongen GA, Verheul HM, et al. PET/CT-derived whole-body and bone marrow dosimetry of ^{89}Zr -cetuximab. *J Nucl Med* 2015;**56**:249–54.
25. Perk LR, Visser GW, Vosjan MJ, Stigter-van Walsum M, Tjink BM, Leemans CR, et al. (^{89}Zr) as a PET surrogate radioisotope for scouting biodistribution of the therapeutic radiometals (^{90}Y) and (^{177}Lu) in tumor-bearing nude mice after coupling to the internalizing antibody cetuximab. *J Nucl Med* 2005;**46**:1898–906.
26. van Dijk LK, Yim CB, Franssen GM, Kaanders JH, Rajander J, Solin O, et al. PET of EGFR with Cu-cetuximab-F(ab') in mice with head and neck squamous cell carcinoma xenografts. *Contrast Media Mol Imaging* 2016;**11**:65–70.
27. Guo Y, Parry JJ, Laforest R, Rogers BE, Anderson CJ. The role of p53 in combination radioimmunotherapy with ^{64}Cu -DOTA-cetuximab and cisplatin in a mouse model of colorectal cancer. *J Nucl Med* 2013;**54**:1621–9.
28. Schechter NR, Wendt 3rd RE, Yang DJ, Azhdarinia A, Erwin WD, Stachowiak AM, et al. Radiation dosimetry of $^{99\text{mTc}}$ -labeled C225 in patients with squamous cell carcinoma of the head and neck. *J Nucl Med* 2004;**45**:1683–7.
29. Rahmim A, Zaidi H. PET versus SPECT: strengths, limitations and challenges. *Nucl Med Commun* 2008;**29**:193–207.
30. Koi L, Bergmann R, Bruchner K, Pietzsch J, Pietzsch HJ, Krause M, et al. Radiolabeled anti-EGFR-antibody improves local tumor control after external beam radiotherapy and offers theragnostic potential. *Radiother Oncol* 2014;**110**:362–9.
31. Gholipour N, Vakili A, Radfar E, Jalilian AR, Bahrani-Samani A, Shirvani-Arani S, et al. Optimization of ^{90}Y -antiCD20 preparation for radioimmunotherapy. *J Cancer Res Ther* 2013;**9**:199–204.
32. Niu G, Sun X, Cao Q, Courter D, Koong A, Le QT, et al. Cetuximab-based immunotherapy and radioimmunotherapy of head and neck squamous cell carcinoma. *Clin Cancer Res* 2010;**16**:2095–105.

33. Ingargiola M, Runge R, Heldt JM, Freudenberg R, Steinbach J, Cordes N, et al. Potential of a Cetuximab-based radioimmunotherapy combined with external irradiation manifests in a 3-D cell assay. *Int J Cancer* 2014;**135**: 968–80.
34. Kareem H, Sandstrom K, Elia R, Gedda L, Anniko M, Lundqvist H, et al. Blocking EGFR in the liver improves the tumor-to-liver uptake ratio of radiolabeled EGF. *Tumour Biol* 2010;**31**:79–87.